Supplementary Information (SI) for Physical Chemistry Chemical Physics.
This journal is © the Owner Societies 2024

Supporting Information

Insights into the Chirality-Dependent Recognition of Danshensu Bingpian Zhi Stereoisomers with PPAR$_\gamma$

Jiasheng Zhao [1, #], Yizhen Zhao [1, #], Shengli Zhang [1], Lei Zhang [1], Zhiwei Yang [1,]*

[1] MOE Key Laboratory for Nonequilibrium Synthesis and Modulation of Condensed Matter, School of Physics, Xi'an Jiaotong University, Xi'an 710049, China

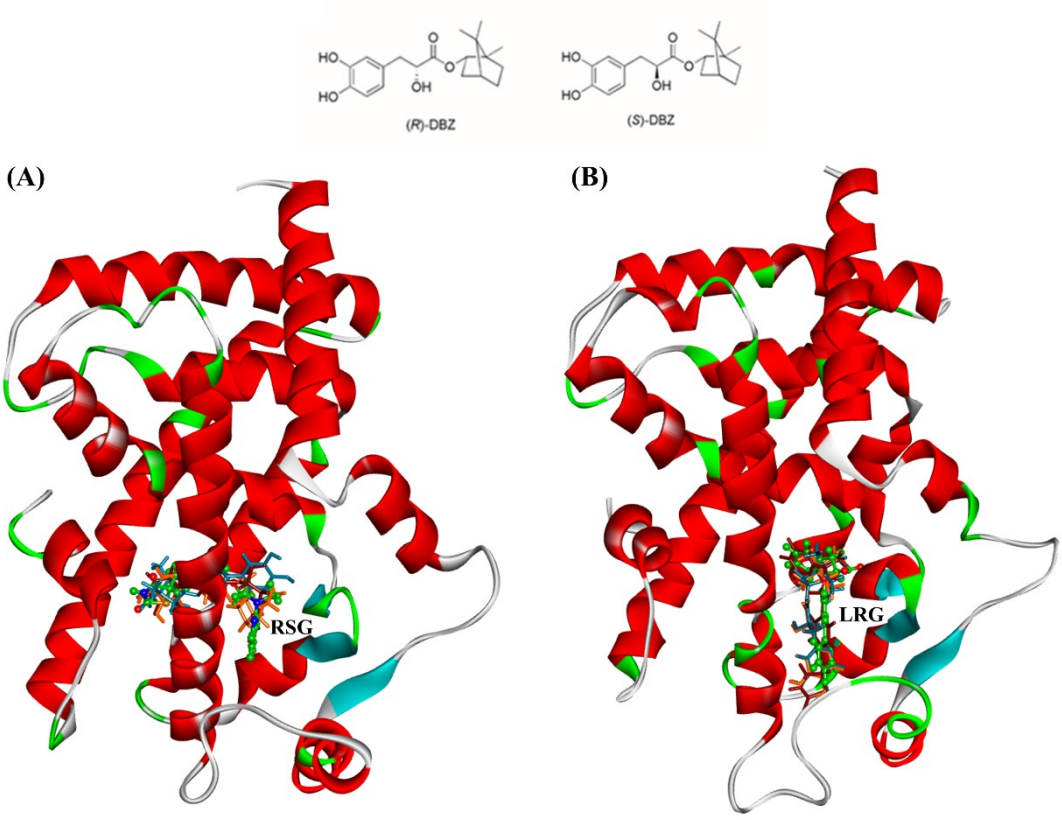

Supplementary Figure 1. Ligands clustered in (A) **Full** and (B) **Partial**. **Full**, full active form of PPAR$_\gamma$-LBD, **Partial**, partial active form of PPAR$_\gamma$-LBD. Ligands are represented by stick models. DBZR and DBZS are able to enter and fill the binding pocket of **Full** and **Partial**. For comparison, the orientation of rosiglitazone (RSG) and (2S)-2-(biphenyl-4-yloxy)-3-phenylpropanoic acid (LRG) are shown in ball and stick models, with O, N, C, S atoms being colored in red, blue, green, and dark yellow, respectively.

[#]These authors contributed equally to this work.
[*]Corresponding author. E-mail: yzws-123@xjtu.edu.cn (ZW Y)

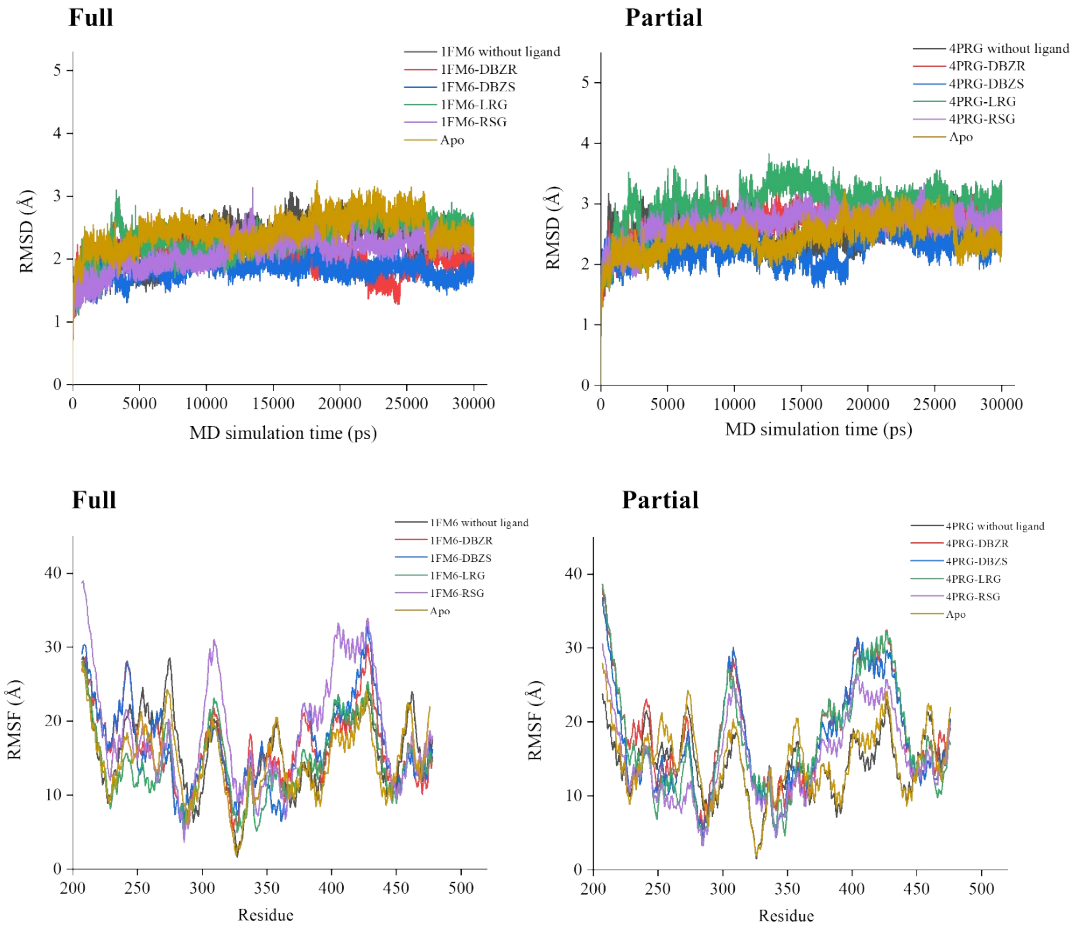

Supplementary Figure 2. Backbone-atom root-mean-square deviations (RMSD) and root-mean-square fluctuations (RMSF) per residues of the **Full** (1FM6) and **Partial** (4PRG)-related systems over the 300-ns MD simulations. The values of apo-active form (**Apo**, 1PRG) are shown as a control simulation of PPAR$_\gamma$-LBD in the absence of ligand.

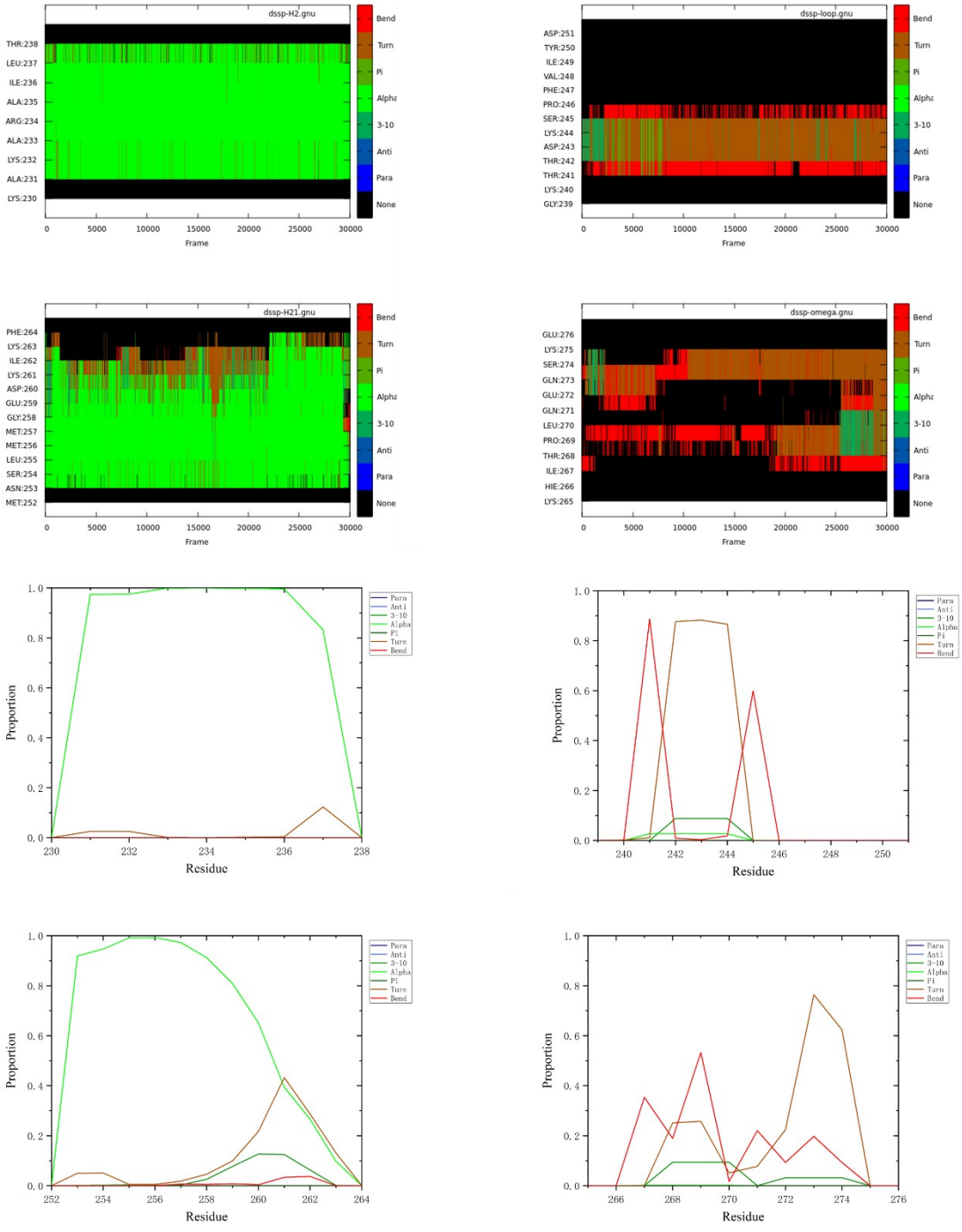

Supplementary Figure 3. Secondary structures of H2 (residues 230-238), S245 loop (residues 239-251), H2′ (residues 252-264) and Ω loop (residues 265-276) in the **Full**-DBZR complex.

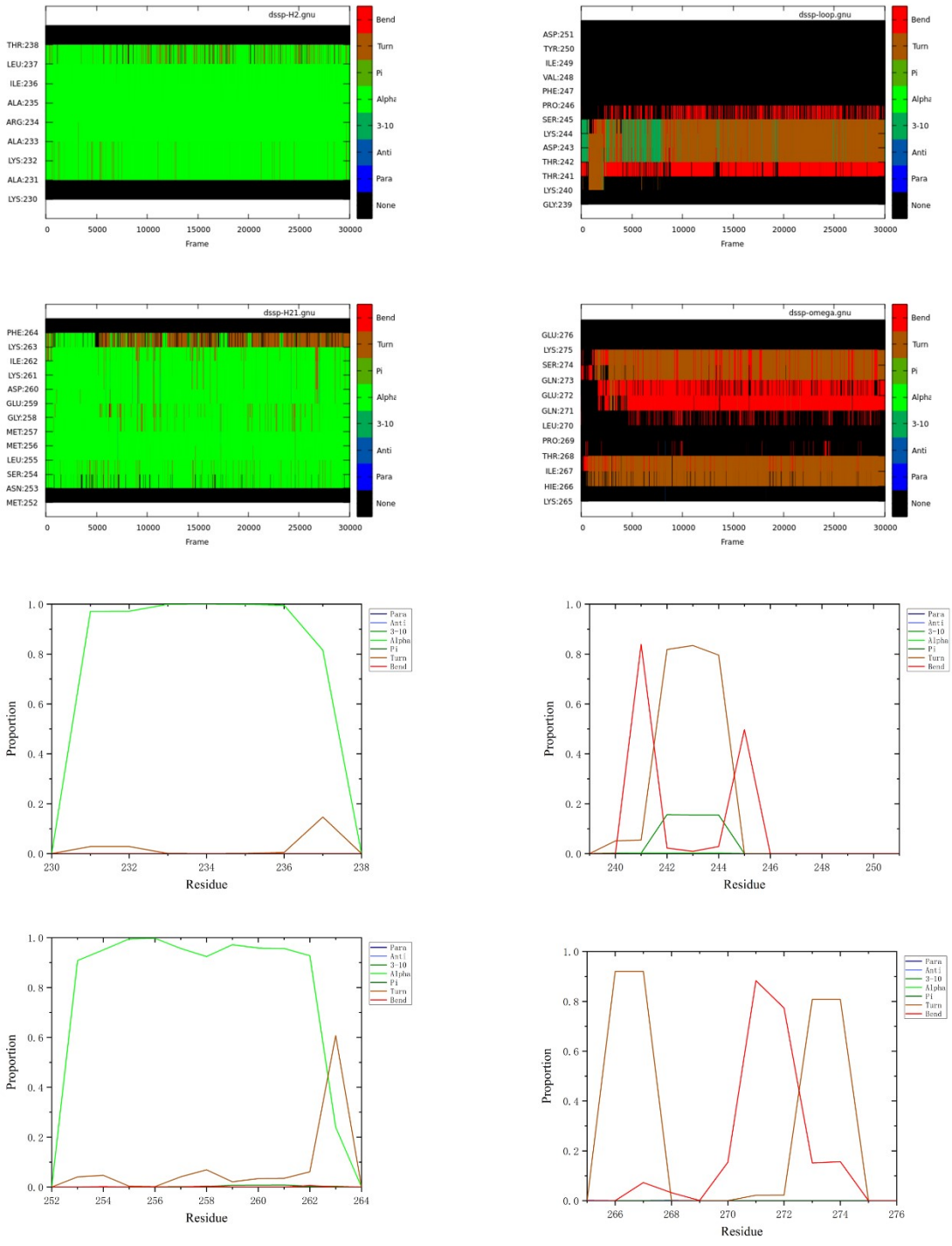

Supplementary Figure 4. Secondary structures of H2 (residues 230-238), S245 loop (residues 239-251), H2′ (residues 252-264) and Ω loop (residues 265-276) in the **Full**-DBZS complex.

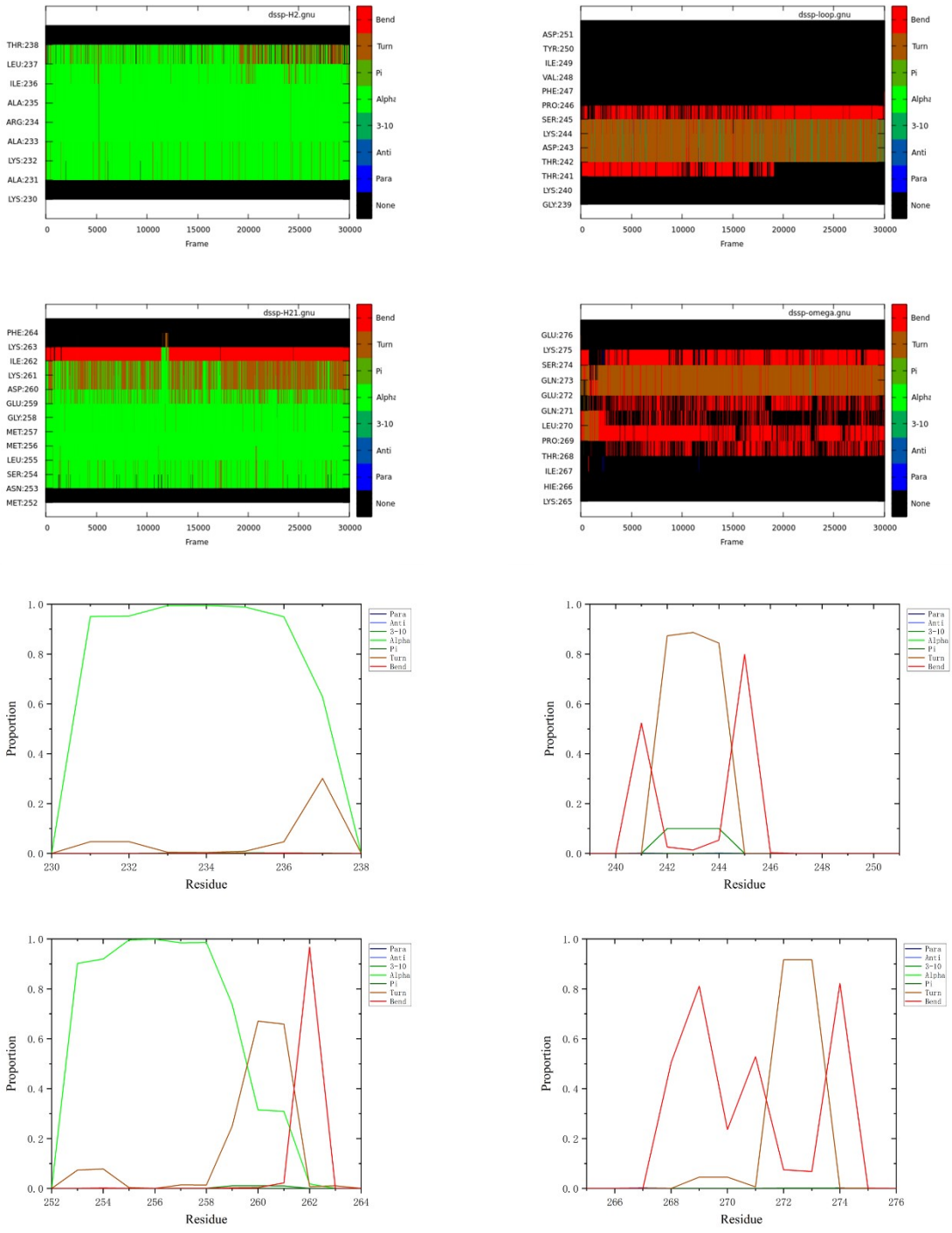

Supplementary Figure 5. Secondary structures of H2 (residues 230-238), S245 loop (residues 239-251), H2′ (residues 252-264) and Ω loop (residues 265-276) in the **Partial-**DBZR complex.

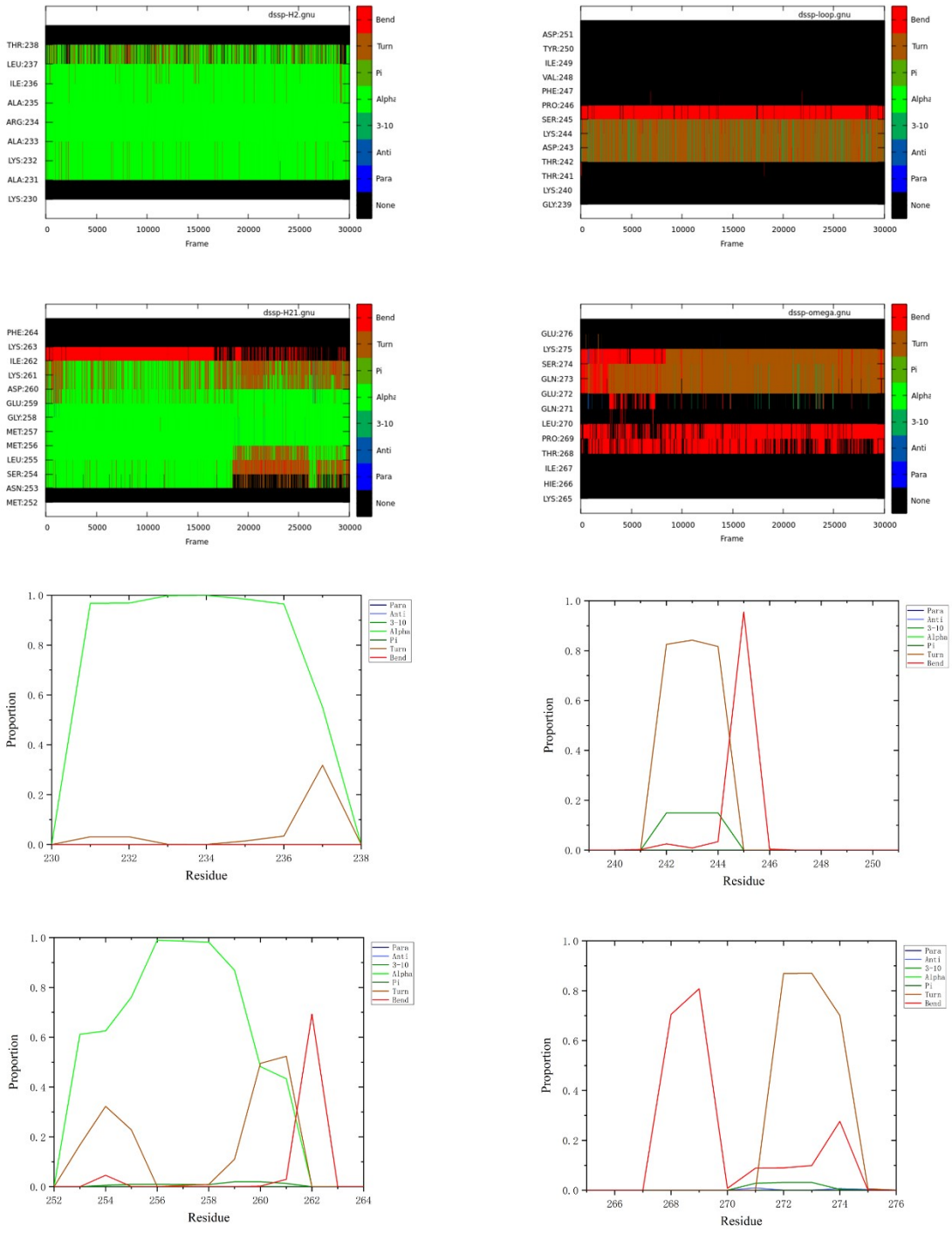

Supplementary Figure 6. Secondary structures of H2 (residues 230-238), S245 loop (residues 239-251), H2′ (residues 252-264) and Ω loop (residues 265-276) in the **Partial**-DBZS complex.

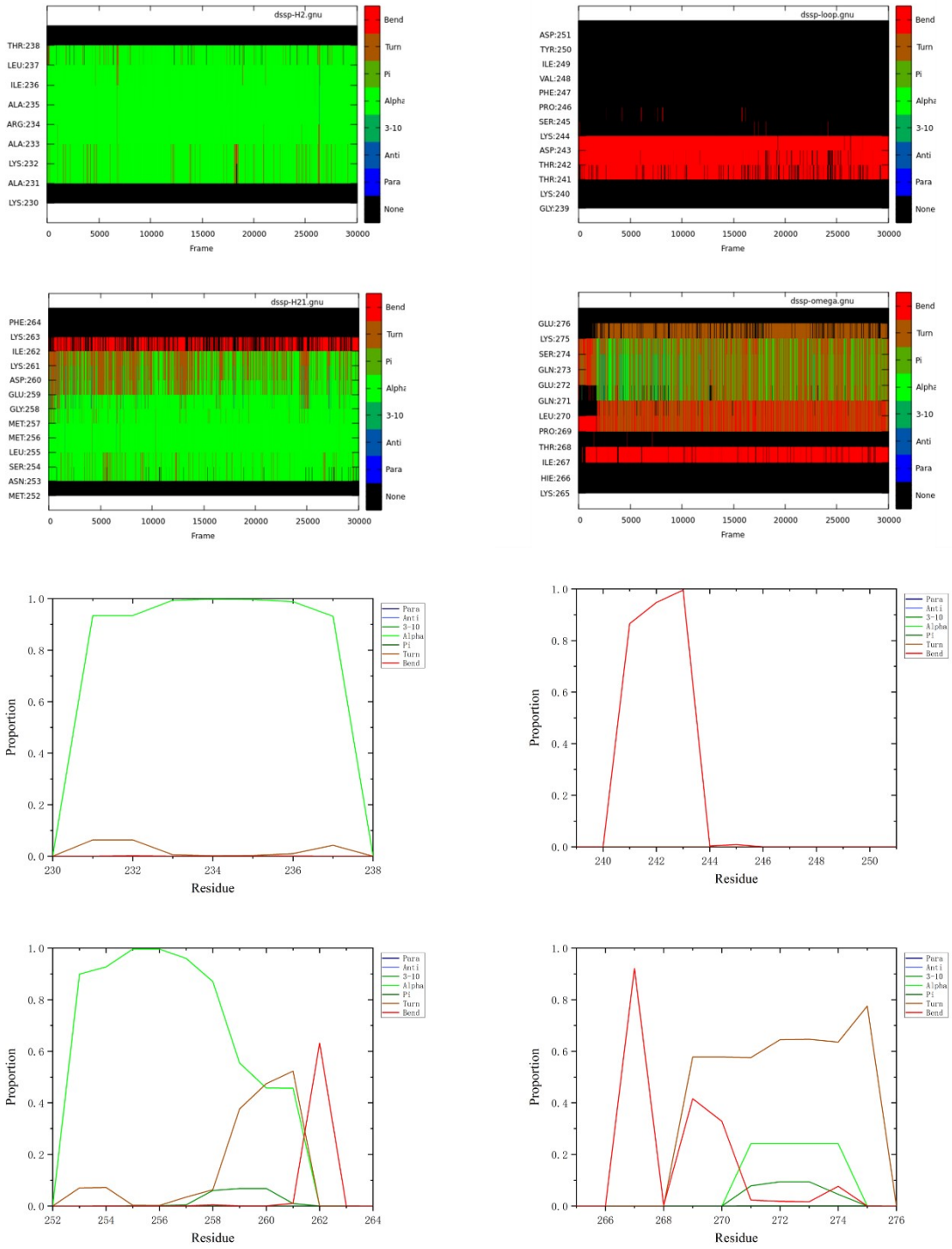

Supplementary Figure 7. Secondary structures of H2 (residues 230-238), S245 loop (residues 239-251), H2′ (residues 252-264) and Ω loop (residues 265-276) in the apo-active form (**Apo**) of PPAR$_\gamma$-LBD (1PRG).

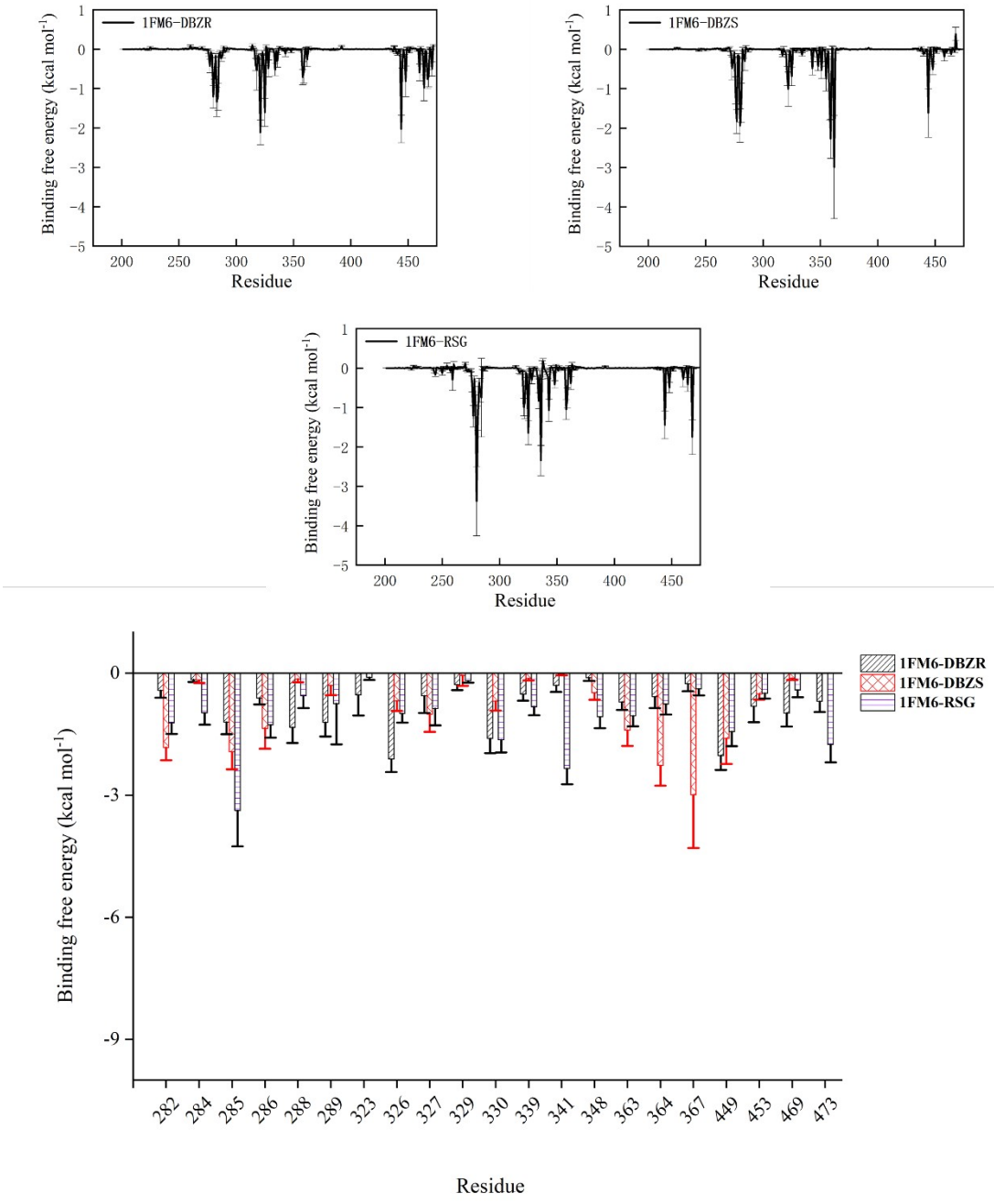

Supplementary Figure 8. Average contribution of the residues to the binding free energies (ΔG_{bind}) within the **Full**-DBZR (in black), **Full**-DBZS (in red) and **Full**-RSG (in blue) complexes. All values are given in kcal·mol^{-1}, with their standard deviations (S.D.).

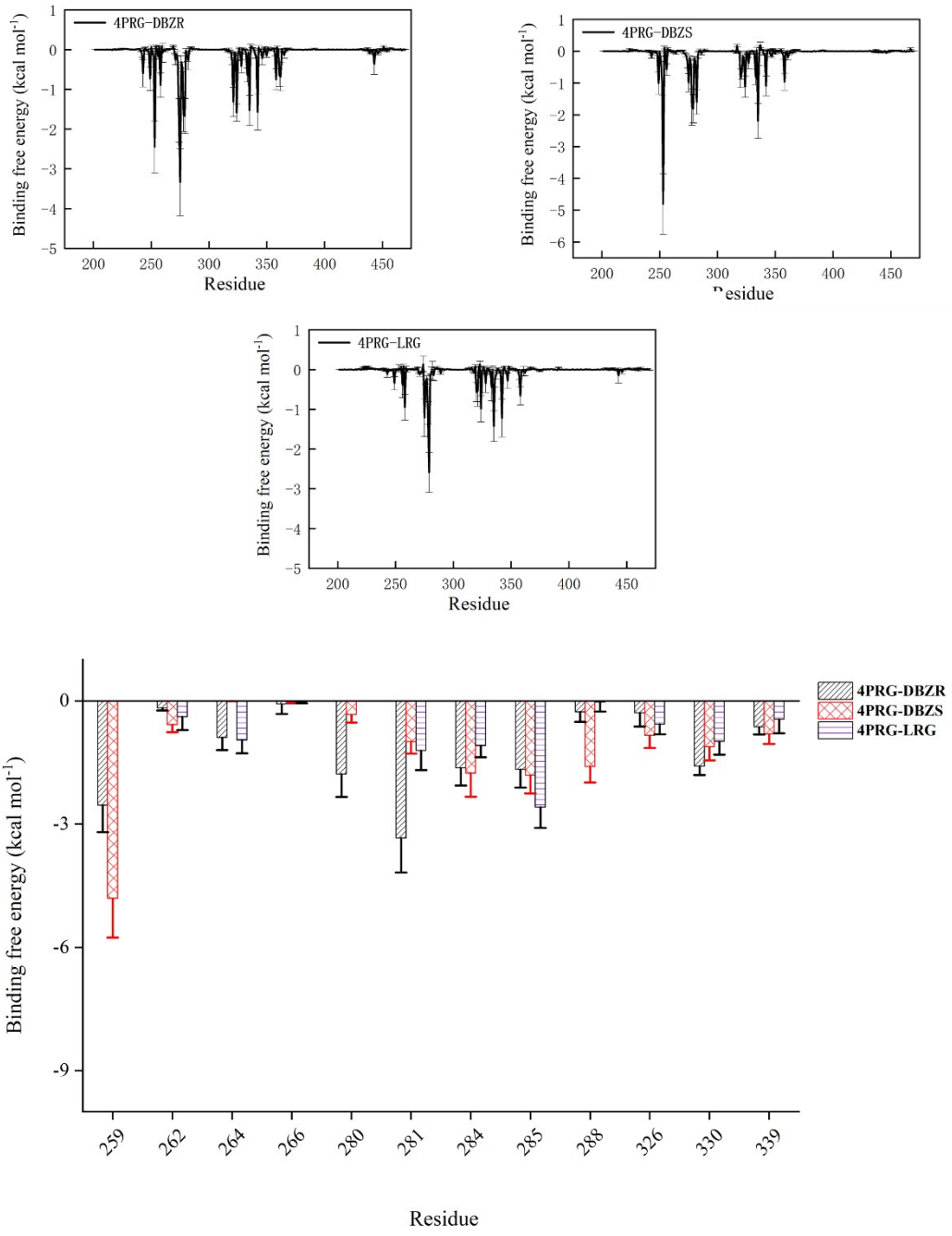

Supplementary Figure 9. Average contribution of the residues to the binding free energies (ΔG_{bind}) within the **Partial**-DBZR (in black), **Partial**-DBZS (in red) and **Partial**-LRG (in blue) complexes. All values are given in kcal·mol^{-1}, with their standard deviations (S.D.).

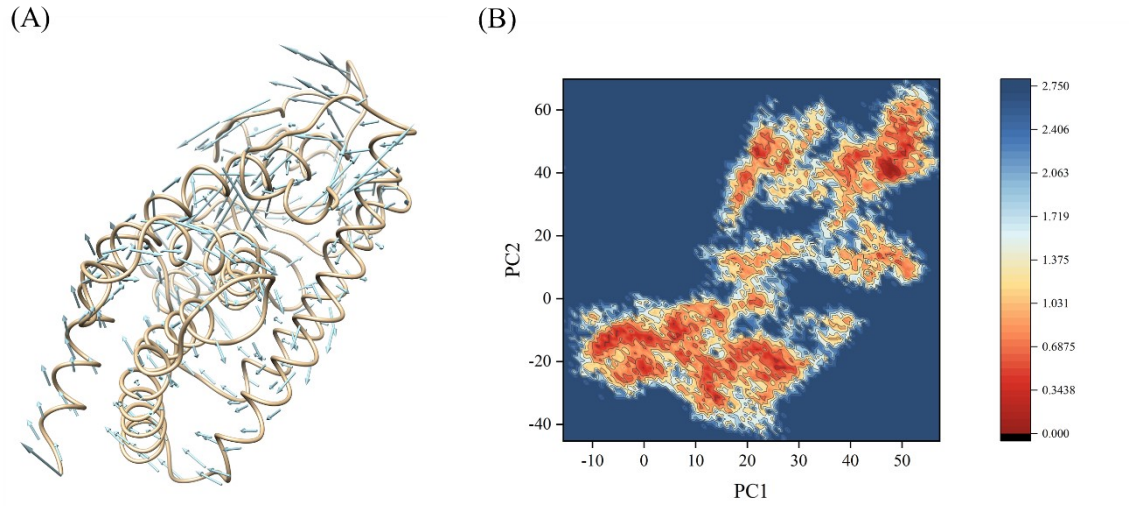

Supplementary Figure 10. Vector field representations of the first principal component (PC) obtained for the protein in the apo-active form (**Apo**) of PPAR$_\gamma$-LBD (1PRG). Conformational landscapes of the protein generated using PC1 and PC2 from the MD simulation.